Electronic Supplementary Material (ESI) for Journal of Materials Chemistry C.

Supporting Information

Solution-based DNA-templating of sub-10nm conductive copper nanowires.

Jonathan Pate,[a] Felix Zamora,[b] Scott M. D. Watson,[a] Nicholas G. Wright,[c] Benjamin R. Horrocks,[a] Andrew Houlton.*[, a]

[a]Chemical Nanoscience Laboratories, School of Chemistry, Bedson Building, Newcastle University, Newcastle upon Tyne, NE1 7RU (UK), [b]Departamento de Quimica Inorgánica Universidad Autónoma de Madrid, 28049 Madrid (Spain), and [c]School of Electrical, Electronic and Computing Engineering, Newcastle University, Newcastle Upon Tyne, NE1 7RU (UK).

Non-templated Cu material

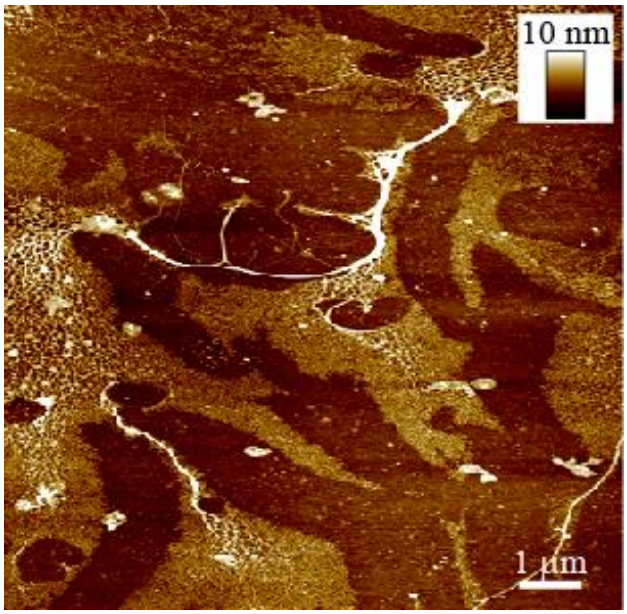

Fig. S1 TappingMode™ AFM height image of material isolated from the top fraction of the DNA/Cu reaction solution following centrifuging at 8000rpm for 2min, and immobilised on a TMS-modified Si wafer. A large amount non-templated Cu material was observed to be present across the wafer surface. This was in contrast to the bottom fraction of the reaction solution, from which only the DNA-templated Cu structures were predominantly observed by AFM.

Thermodynamic model of templated growth

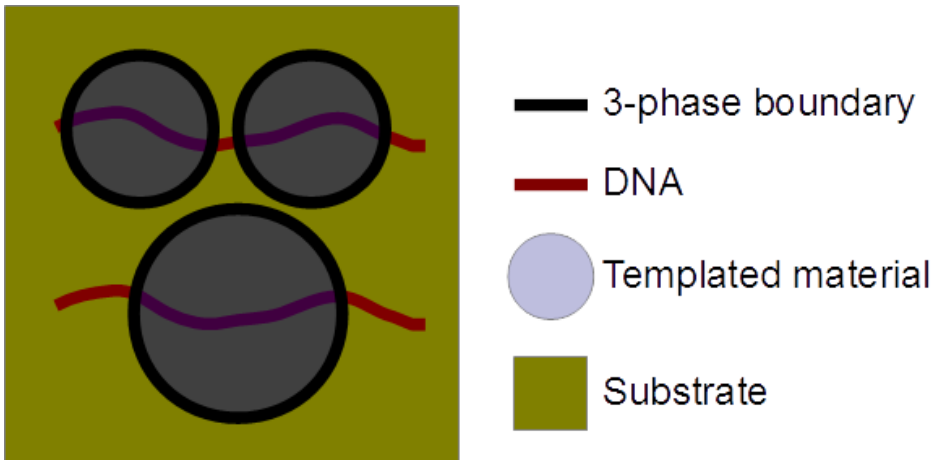

Fig. S2 Cartoon illustration, highlighting the additional terms in the free energy that must be considered when templating on surface-immobilised DNA: (i) adhesion of the material to the substrate and (ii) the line energy at the 3-phase boundary.

UV-vis spectroscopy

Due to the need for milliliter-scale quantities of the templating solutions in order to measure the optical absorption spectra, calf thymus (CT) DNA was used which can be readily obtained from commercial sources in sufficiently large quantities. UV-vis absorption spectra were acquired using a Varian Cary-100 Bio UV-vis spectrometer. Measurements were carried out upon solutions of CT-DNA (300μg/mL, 870 μL), to which a solution of $Cu(NO_3)_2.3H_2O$ (aq. 500μM, 120μL) was added drop-wise. Ascorbic acid (aq. 0.12M, 10μL) was subsequently added to the solution, and the absorption measurement repeated.

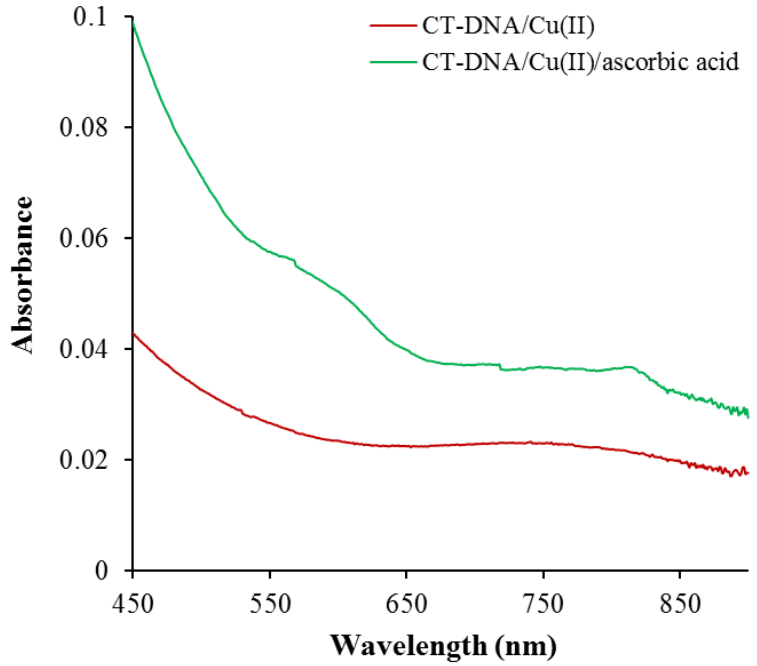

Fig. S3 UV-vis absorption spectra of aqueous solutions containing CT-DNA/Cu(II) (red), and CT-DNA/Cu(II)/ascorbic acid (green). The absorption band at ~790nm in the CT-DNA/Cu(II) spectrum is attributed to Cu(II) d-d transitions. Upon addition of ascorbic acid to the solution (green spectrum), a broad plasmon resonance band between 540-630nm was observed, correlating with the formation of nanostructured Cu(0) materials in the solution.

FTIR

FTIR spectra were recorded in transmission mode on a Bio-Rad Excalibur FTS-40 spectrometer (Varian., Palo Alto, CA) equipped with a liquid nitrogen cooled deuterated triglycine sulfate (DTGS) detector. Spectra were collected at 512 scans, and 2cm^{-1} resolution.

Samples were prepared by mixing solutions of CT-DNA (aq. 300µg/mL, 250µL) and $Cu(NO_3)_2.3H_2O$ (aq. 50µM, 250µL), followed by drop wise addition of ascorbic acid (aq. 2mM, 250µL). The reaction solution was left to incubate at room temperature, whilst stirring on a mechanical roller, for 3hr. Following this time period the solution was centrifuged at 8000rpm for 2min in order to separate the suspension of nanowires from non-templated Cu nanoparticles also formed in the reaction solution. 60µL of the nanowire suspension was deposited onto a clean Si<n-100> wafer (Piranha-treated) and left to dry. This deposition procedure was repeated a further two times on the wafer to ensure there was sufficient material present to obtain a spectrum.

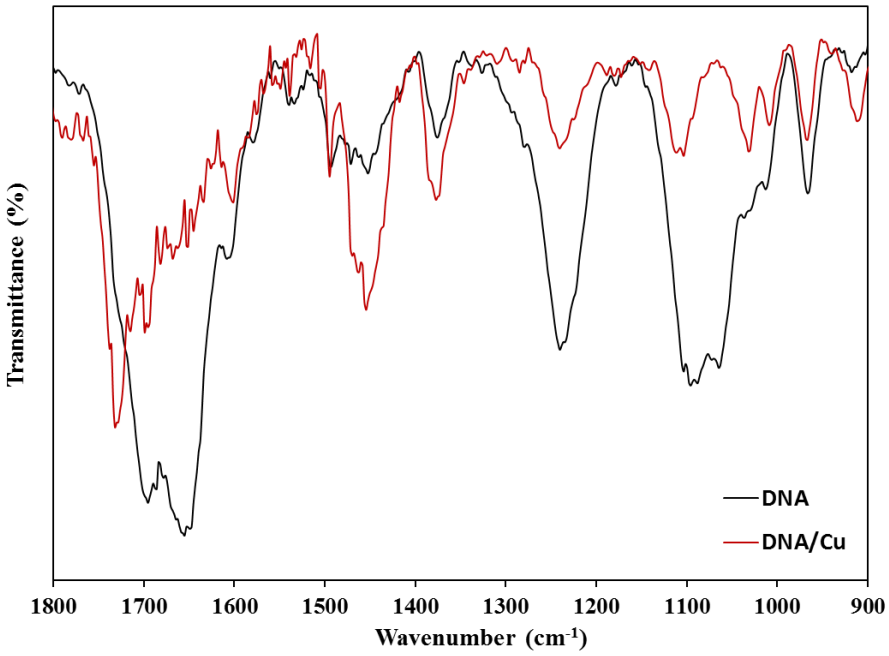

Fig. S4 FTIR spectra of bare CT-DNA (black spectrum) and CT-DNA following metallization with Cu.

Table S1 Assignments of bands in FTIR spectra of bare CT-DNA and Cu-metallized CT-DNA (shown in Figure S1). Band assignments were made based upon previous literature values.[1-4]

Assignment	**Wavenumber (cm^{-1})**	
	CT-DNA	**CT-DNA/Cu**
C6=O stretch of guanine	1696	1728
C2=O stretch of cytosine	1655	1695
C=N cytosine; N-H adenine; C7=N adenine	1607	1602
C=N guanine and adenine stretch	1578	-
In-plane vibration of guanine and cytosine	1534	1539
C8-N coupled with a ring vibration of guanine	1491	1493
C-N stretch of thymine, guanine and cytosine	1452	1452
C-N stretch of guanine and cytosine	1376	1377
C-N stretch of adenine	1326	-
PO_2^- asymmetric stretch	1238	1238
PO_2^- symmetric stretch	1097	1104
P-O or C-O symmetric stretch	1064	1031
C-O deoxyribose stretch	1013	1009
C-C deoxyribose stretch	966	967

Powder X-ray diffraction

Powder samples for XRD analysis were prepared by mixing solutions of CT-DNA (aq. 1 mg/mL, 10mL) and $Cu(NO_3)_2.3H_2O$ (aq. 0.5M, 10mL), followed by the drop wise addition of a solution of ascorbic acid (aq. 1.0M, 20mL). High concentrations of the reagents in the templating solution were necessary here in order for the product material to form as a powder. Upon addition of the ascorbic acid solution, an immediate colour change in the solution from blue to green was observed. The reaction solution was left to stir overnight at room temperature after which a small amount of red precipitate was present. The mixture was then placed in a refrigerator for a further 24hr during which time more red precipitate formed. To isolate the product material, the sample was centrifuged at 8000rpm for 30min, after which the supernatant was decanted and the red solid was collected and serially washed with NANOpure® water and ethanol before drying under vacuum. Powder X-ray diffraction data was obtained using a PANalytical X'Pert Pro Diffractomer equipped with a Cu $K\alpha_1$ radiation source ($\lambda = 1.54 \times 10^{-10}$m).

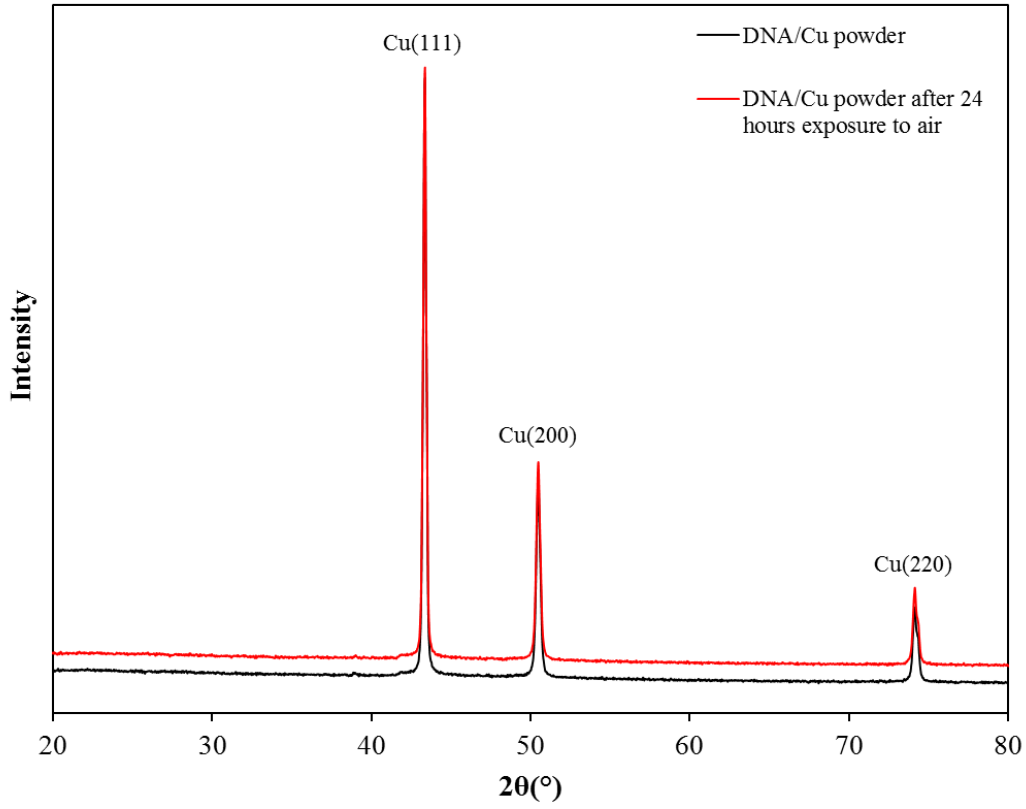

Fig. S5 XRD pattern of a powder sample of CT-DNA-templated Cu material (black), and the same sample following exposure to air for 24hr (red). The three diffraction peaks at 2θ values of 43.4°, 50.5°, 74.1° are consistent with the reflections associated with metallic Cu(0).[5-7] No additional peaks, associated with impurities (*e.g.* oxides of the Cu) were identified. No changes were observed in the diffraction pattern following exposure of the sample to air for 24hr, confirming that no significant oxidation of the material has taken place over this time period.

X-ray photoelectron spectroscopy

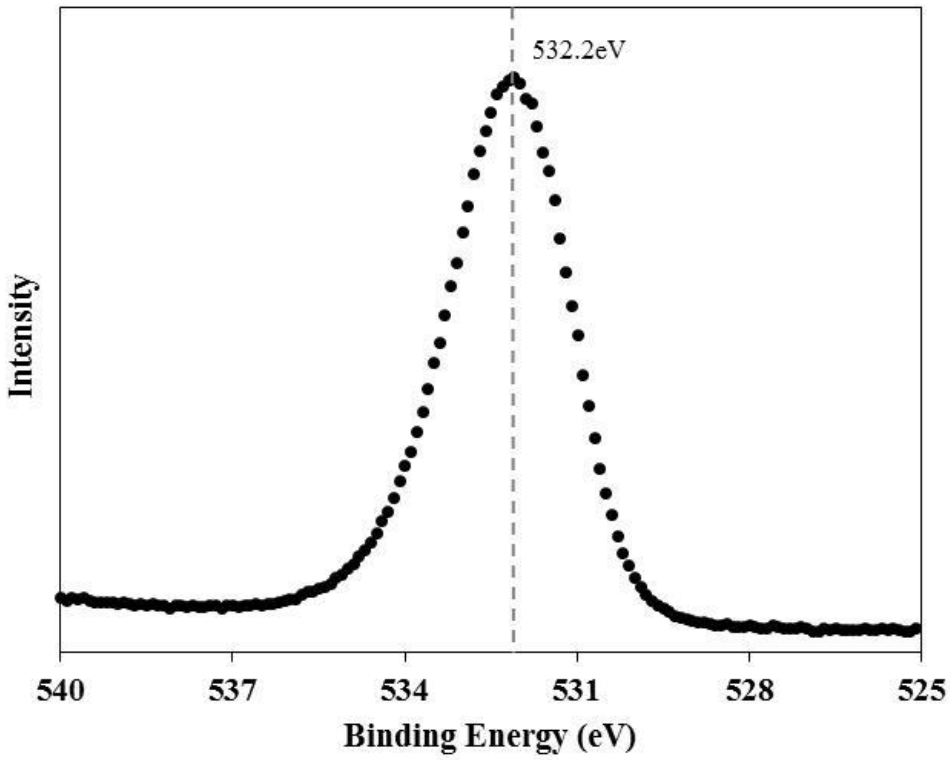

Fig. S6 High-resolution XP spectrum of O1s region collected from a sample of DNA-templated Cu nanowires. Contributions to the O1s spectrum are expected to arise from the support substrate (Si/SiO_2 wafer), DNA (phosphate backbone, sugar, and bases), and the NO_3^- species originating from the $Cu(NO_3)_2$ starting material.[8-14]

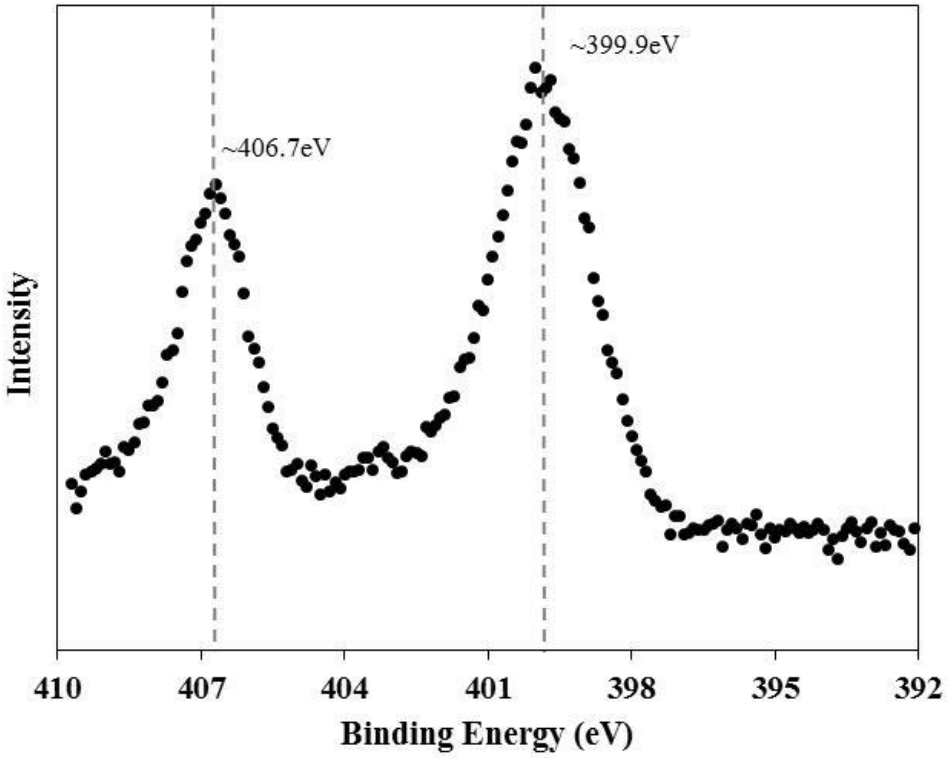

Fig. S7 High-resolution XP spectrum of N1s region collected from a sample of DNA-templated Cu nanowires. Two distinct peaks are shown around ~399.9eV and ~406.7eV. The lower binding energy peak corresponds to the region where nitrogen present in DNA would be expected to be observed, whilst the peak at much higher binding energy falls within the expected region for NO_3^- anions.[13-15] The presence of NO_3^- in the sample can be related to the $Cu(NO_3)_2$ starting material used in the DNA/Cu nanowire fabrication method.

AFM

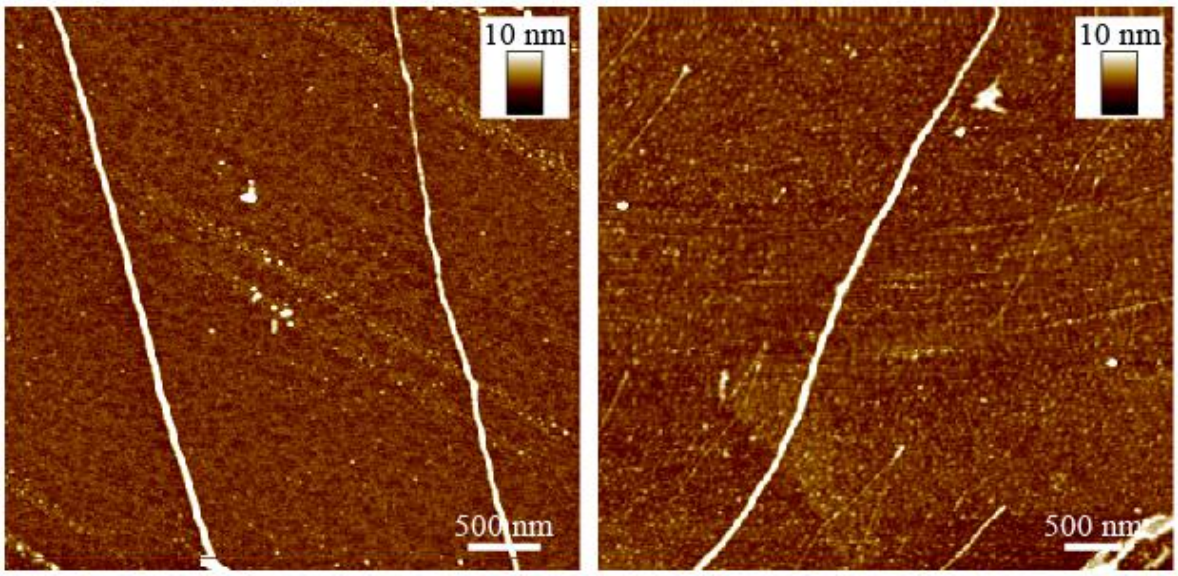

Fig. S8 TappingMode™ AFM height images of further examples of DNA-templated Cu nanowires, aligned upon TMS-modified Si wafers. The nanowires were prepared under the appropriate reaction conditions, established for producing DNA/Cu structures which possess smooth and continuous Cu coatings around the DNA template, as discussed in the manuscript.

Scanning conductance microscopy

The relationship between the measured nanowire phase shifts and applied bias also allows us to identify the dominant interactions which occur between the tip and sample during SCM experiments. SCM is primarily sensitive to two types of tip–sample interaction: (i) capacitance effects, where the phase shift dependence on the applied bias is parabolic (*i.e.* proportional to V^2) and (ii) trapped charge effects where the phase shift dependence is linear (*i.e.* proportional to V). The parabolic shape of the 'phase shift *vs.* applied bias' plot (see Fig. S9), corresponding to main DNA/Cu structure shown in Fig. 4 (white arrow) in the manuscript, indicates that the tip–sample interactions were dominated by capacitance effects (though the slight asymmetry seen can be attributed to a small contribution from trapped charges).

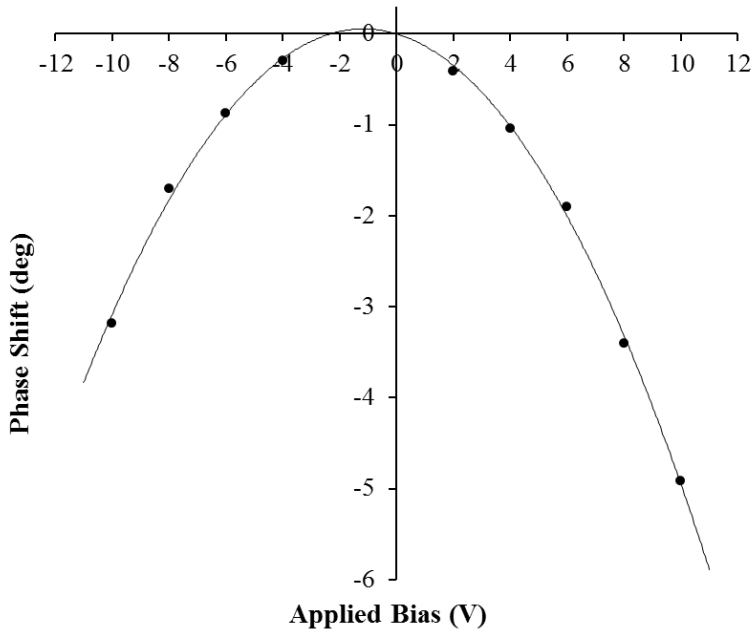

Fig. S9 Plot showing measured SCM phase shifts associated with the DNA-templated Cu structure shown in Fig. 4 (white arrow) in the manuscript, as a function of the applied dc sample bias. The negative sign associated with the phase shifts, along with the parabolic shape of the plot, are characteristic of the DNA/Cu structure being electrically conducting, and the tip–sample interactions being dominated by capacitance effects.

cAFM

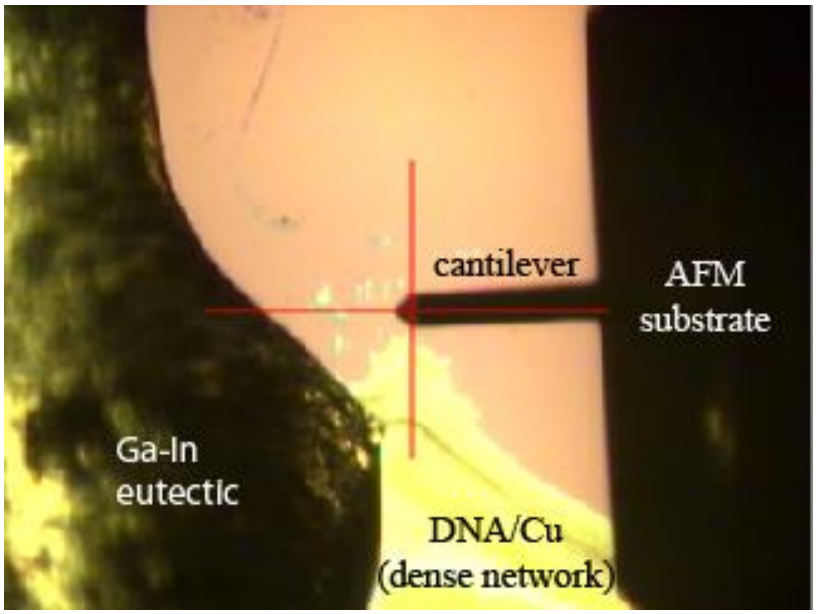

Fig. S10 Optical image of the experimental setup used for carrying out cAFM measurements upon samples of DNA-templated Cu structures. The image shows the DNA/Cu nanowire network, the Ga-In eutectic used to provide an electrical connection between the nanowire network and the AFM sample chuck, and the position of AFM cantilever at the edge of network where cAFM measurements were typically performed.

References

1. S. Alex and P. Dupuis, *Inorganica Chimica Acta*, 1989, **157**, 271-281.
2. A. A. Ouameur and H. A. Tajmir-Riahi, *Journal of Biological Chemistry*, 2004, **279**, 42041-42054.
3. H. Arakawa, R. Ahmad, M. Naoui and H. A. Tajmir-Riahi, *Journal of Biological Chemistry*, 2000, **275**, 10150-10153.
4. G. I. Dovbeshko, N. Y. Gridina, E. B. Kruglova and O. P. Pashchuk, *Talanta*, 2000, **53**, 233-246.
5. M. Mohl, P. Pusztai, A. Kukovecz, Z. Konya, J. Kukkola, K. Kordas, R. Vajtai and P. M. Ajayan, *Langmuir*, 2010, **26**, 16496-16502.
6. J. L. C. Huaman, K. Sato, S. Kurita, T. Matsumoto and B. Jeyadevan, *J. Mater. Chem.*, 2011, **21**, 7062-7069.
7. Z. Liu, Y. Yang, J. Liang, Z. Hu, S. Li, S. Peng and Y. Qian, *J. Phys. Chem. B*, 2003, **107**, 12658-12661.
8. M. R. Vilar, A. M. Botelho do Rego, A. M. Ferraria, Y. Jugnet, C. Noguès, D. Peled and R. Naaman, *J. Phys. Chem. B*, 2008, **112**, 6957-6964.
9. C.-Y. Lee, P. Gong, G. M. Harbers, D. W. Grainger, D. G. Castner and L. J. Gamble, *Anal. Chem.*, 2006, **78**, 3316-3325.
10. G. Hollinger, Y. Jugnet, P. Pertosa and T. M. Duc, *Chem. Phys. Lett.*, 1975, **36**, 441-445.
11. R. P. Netterfield, P. J. Martin, C. G. Pacey, W. G. Sainty, D. R. McKenzie and G. Auchterlonie, *J. Appl. Phys.*, 1989, **66**, 1805-1809.
12. M. L. Miller and R. W. Linton, *Anal. Chem.*, 1985, **57**, 2314-2319.
13. R. P. Vasquez, *J. Electron Spectrosc. Relat. Phenom.*, 1991, **56**, 217-240.
14. C. E. Nanayakkara, P. M. Jayaweera, G. Rubasingehege, J. Baltrusaitis and V. H. Grassian, *J. Phys. Chem. A*, 2014, **118**, 158-166.
15. J. Baltrusaitis, P. M. Jayaweera and V. H. Grassian, *Phys. Chem. Chem. Phys.*, 2009, **11**, 8295-8305.